ACS APPLIED MATERIALS & INTERFACES

Research Article

www.acsami.org

Layer-by-Layer Modification of Cation Exchange Membranes Controls Ion Selectivity and Water Splitting

Said Abdu,[†,⊥] Manuel-César Martí-Calatayud,[†,‡,⊥] John Erik Wong,[†,§] Montserrat García-Gabaldón,[‡] and Matthias Wessling*[,†,§]

[†]Chemical Process Engineering, RWTH Aachen University, Turmstr. 46, 52064 Aachen, Germany

[‡]Electrochemical Engineering & Corrosion Group (IEC), Departament d'Enginyeria Química i Nuclear, Universitat Politècnica de València, P.O. Box 22012, 46071 València, Spain

[§]DWI - Leibniz Institute for Interactive Materials, Forckenbeckstraße 50, 52056 Aachen, Germany

Supporting Information

ABSTRACT: The present study investigates the possibility of inducing monovalent ion permselectivity on standard cation exchange membranes, by the layer-by-layer (LbL) assembly of poly(ethyleneimine) (PEI)/poly(styrenesulfonate) (PSS) polyelectrolyte multilayers. Coating of the $(PEI/PSS)_N$ LbL multilayers on the CMX membrane caused only moderate variation of the ohmic resistance of the membrane systems. Nonetheless, the polyelectrolyte multilayers had a substantial influence on the monovalent ion permselectivity of the membranes. Permselectivity comparable to that of a commercial monovalent-ion-permselective membrane was obtained with only six bilayers of polyelectrolytes, yet with significantly lower energy consumption per mole of Na^+ ions transported through the membranes. The monovalent ion permselectivity stems from an increased Donnan exclusion for divalent ions and hydrophobization of the surface of the membranes concomitant to their modification. Double-layer capacitance obtained from impedance measurements shows a qualitative indication of the divalent ion repulsion of the membranes. At overlimiting current densities, water dissociation occurred at membranes with PEI-terminated layers and increased with the number of layers, while it was nearly absent for the PSS-terminated layers. Hence, LbL layers allow switching on and turning off water splitting at the surface of ion exchange membranes.

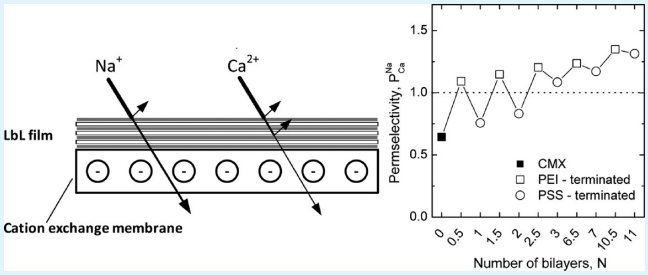

KEYWORDS: *electrodialysis, cation exchange membrane, monovalent ion permselectivity, water splitting, layer-by-layer, polyelectrolyte*

1. INTRODUCTION

Electrodialysis is an electrochemical separation technology used to separate inorganic salts from aqueous environments to desalinate water and treat wastewater.[1] It is also applied to separate solutions containing organic ionic species.[2] The heart of electrodialysis processes is ion exchange membranes which selectively pass ions of opposite charge under the application of an electric field. These membranes consist of polymeric films bearing covalently bound ionic fixed charges which enable the transport of the electrolyte ions with opposite charge sign (counterions) through the membrane structure. Ions with the same charge sign (co-ions) are electrostatically repelled and retained in the feed compartment. This technology can be integrated in industrial processes in which the separation of ions to recover valuable products is desired. Furthermore, the development of ion exchange membranes with increased permselectivity for specific ions may extend the applicability of electrodialysis to more demanding operations. In this regard, an important progress in the field of membrane technology is the development of membranes selective to monovalent ions, i.e., membranes capable of separating ions with the same charge sign but different valence.

Monovalent-ion-permselective membranes are of special utility for those applications in which monovalent cations are the product of interest to be separated from mixtures with multivalent ions. A large-scale application of this type of membranes has already been realized for the purpose of edible salt production from seawater, where multivalent ions are undesired in the product and scale formation on the membranes is prevented by rejecting the multivalent ions.[3] Other emerging applications include the recovery of spent acids generated in metal finishing industries,[4] hardness removal to produce drinking water,[5] and electrochemical acidification of milk.[6,7]

Several aspects determine the permselectivity of ion-conducting membranes for cations of different valence. First, the affinity under equilibrium conditions between the fixed

Received: October 30, 2013
Accepted: January 8, 2014
Published: January 8, 2014

Table 1. Measured Properties of the Used Commercial Ion Exchange Membranes

name	trademark	type	ion exchange capacity (meq/g)	membrane thickness in swollen state (mm)	area resistance ($\Omega \cdot cm^2$)[a]
CMX	Neosepta	standard	1.66	0.16	3.50
CMS	Neosepta	monovalent-ion-selective	2.30	0.13	3.49
CSO	Selemion	monovalent-ion-selective	2.55	0.09	4.09

[a]Equilibrated in 0.5 M NaCl, measured at 25 °C.

charges of the membranes and the solution counterions is strongly affected by electrostatic forces, so that the fixed ion exchange sites have usually larger attraction toward multivalent cations.[8] Another important factor is the size and mobility of ions under the application of current since the membrane structure could retard the transport of cations of larger size. In addition, depending on the applied current density and the hydrodynamic conditions the properties of the diffusion boundary layer developed near the membrane surface can favor the supply of specific cations from the bulk solution to the membrane surface.[8−10]

Therefore, taking into account the above factors, different approaches can be considered to increase the membrane permselectivity for monovalent cations. An increased monovalent permselectivity can be induced by increasing the membrane's cross-linking density and making the membrane matrix denser, which hinders the diffusion of large ions through the membrane structure.[11,12] Alternatively, the deposition of a thin positively charged layer on the surface of cationic membranes has been applied to increase the repulsion toward multivalent species. The latter methodology entails an additional advantage since the electrostatic repulsion of multivalent ions would also prevent the formation of precipitates of multivalent metal species on the membrane surface, thus acting as an antifouling mechanism.[13,14]

The deposition of a thin layer of cationic polyelectrolytes on the surface of membranes has been previously accomplished in different studies.[4,15,16] However, new approaches are needed to further increase the membrane permselectivity and avoid problems related to the deterioration of the adsorbed films.[15,17,18] To this end, utilization of the layer-by-layer (LbL) assembly of polyelectrolyte multilayers, as a facile and precise method to tailor and control the electrostatic properties of the membrane surface, arises as a viable and promising alternative to obtain highly monovalent-ion-permselective membranes.[19] An increase in the proportion of positively charged groups on the membrane active layer can be obtained by using such a procedure, which is based on the alternate dipping of the cation exchange membrane in polycations and polyanions. With the first deposition step, electrostatic attractions anchor the first polyelectrolyte layer on the oppositely charged membrane surface. Simultaneously, a charge reversal of the membrane surface occurs, thus leaving the surface prepared for the next adsorption step.[20] The adhesion of the subsequent polyelectrolyte layer is ensured through a high number of electrostatic bonds created with the opposite charges of the previously deposited polyelectrolyte. In this manner, the thickness and functional properties of the membrane coating can be finely tuned by adjusting the adsorption parameters and the number of deposited bilayers.

In the field of membrane technology, this methodology has been recently applied to increase the solvent stability of nanofiltration membranes while maintaining good retention and permeability.[21] Previously we modified ultrafiltration membranes by LbL assembly without any prior treatment of their surface,[22] and more recently we reported the successful catalysis of water splitting in bipolar membranes via polyelectrolyte multilayers.[23] The performance of ion exchange membranes used in direct methanol fuel cells has also been improved, by reducing the methanol crossover with LbL polyelectrolyte assemblies.[24] Other studies report the increase of the multivalent ion rejection of pressure-driven as well as anion exchange membranes after being modified with polyelectrolyte coatings.[13,25]

In the present study, the LbL procedure was aimed to increase the monovalent permselectivity of cation exchange membranes. The modified membranes were characterized by several surface analytical methods, and their surface characteristics were correlated with their electrochemical transport behavior. Their performance was investigated and compared with that of other commercial membranes by galvanostatic permselectivity experiments, current−voltage curves, and electrochemical impedance spectroscopy (EIS) measurements.

2. EXPERIMENTAL SECTION

2.1. Membranes, Materials, and Reagents. The membranes used in the experiments were either commercial cation exchange membranes or modified membranes. Properties of the commercial membranes are shown in Table 1.

CMX (Astom, Japan) is a standard cation exchange membrane used for electrodialysis. CMS (Astom, Japan) and CSO (Asahi Glass, Japan) are monovalent-ion-permselective cation exchange membranes. CMS features monovalent ion permselectivity on both of its sides, whereas CSO is designated with an active side.

The LbL multilayers were formed from the following polyelectrolytes: poly(ethyleneimine) (PEI), molecular weight (MW) = 750 000 g/mol, and poly(4-styrenesulfonate) (PSS), MW = 70 000 g/mol. They were both obtained from Sigma-Aldrich and were dissolved in ultrapure water.

Synthetic solutions mixing 0.05 M NaCl and 0.05 M $CaCl_2$ (reagent grade dissolved in DI water) were used for electrochemical characterization of the membranes.

2.2. Membrane Modification. PEI and PSS were selected to form the polyelectrolyte multilayers on the surface of the membranes. PSS was selected as the polyanion because it is a strong polyelectrolyte and PEI as the polycation due to its hyperbranched structure and the high density of its positively charged amine groups. Their chemical structures are shown in Figure 1(a) and (b), respectively.

To introduce the polyelectrolyte multilayers, the CMX membrane was first rinsed with ultrapure water and coated on one side with the

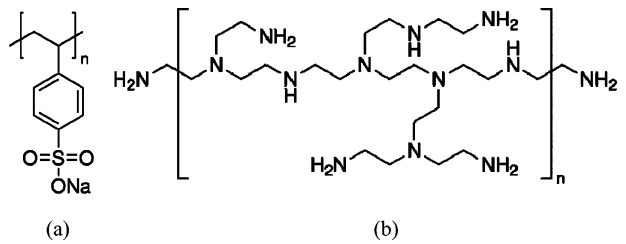

(a) (b)

Figure 1. Chemical structure of (a) poly(4-styrenesulfonate) (PSS) and (b) hyperbranched poly(ethyleneimine) (PEI).

desired polyelectrolyte multilayers. The membrane was prior to that stored in 0.5 M NaCl solution. The coating was carried out in an in-house-built coating cell by the LbL assembly method. First the CMX was exposed to a 1 g/L solution of PEI for 1 h, followed by 1 g/L PSS solution for 30 min. Except the first layer, where the membrane was brought into contact with PEI for 1 h, the rest of the layers were formed each for 30 min, PEI as well as PSS. In between the coating steps, the membranes were thoroughly rinsed with ultrapure water. The polyelectrolytes formed the active side on the CMX membrane—the side that faces the anode in subsequent experiments.

The nomenclature employed to designate the modified membranes is the following: $(CMX)/(PEI/PSS)_N$. The term CMX indicates the substrate membrane, PEI and PSS the polycation and the polyanion, respectively, and the subscript N the number of bilayers. Unless mentioned otherwise, both the PEI and PSS were prepared in ultrapure water.

2.3. Surface Characterization of the Membranes. The deposition of the polyelectrolyte layers was monitored by contact angle measurements (Krüss, DSA10-MK2) and X-ray photoelectron spectroscopy (XPS) (Kratos Analytical, Axis Ultra). Furthermore, the deposited polyelectrolyte multilayers were visually characterized using field emission-scanning electron microscopy (FE-SEM) (Hitachi, S-4800).

The contact angle measurements were performed, immediately after modification. The images for analysis of the contact angles were taken 1 min after the water droplet had settled on the membrane surface. For each membrane an average of at least five measurements of the contact angle was taken, measured at different locations of the samples. The contact angle was evaluated by the sessile drop method.

2.4. Electrochemical Characterization of the Membranes. Polarization current–voltage curves and impedance spectra were obtained to characterize the electrochemical behavior of the modified membranes. The measurements were performed in a six-compartment electrodialytic cell shown schematically in Figure 2. The membrane to be investigated was placed in the middle of the cell. The other membranes (Neosepta AMX and CMX) are auxiliary membranes, used to limit interference of the electrode reactions on the measurement. The membranes were characterized in 0.05 M equimolar mixtures of chloride salts of mono- and divalent cations (Na^+ and Ca^{2+} ions). Prior to that, the membranes were conditioned in the salt solution (0.05 M NaCl and 0.05 M $CaCl_2$) for about 24 h outside the membrane module.

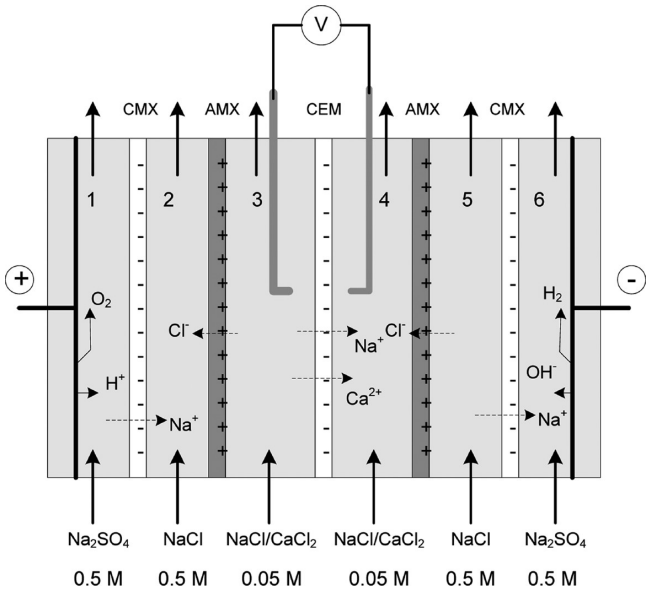

Figure 2. Schematic drawing of a six-compartment measurement module for polarization curves, permselectivity, and impedance measurements.

The DC current–voltage measurements were performed with each commercial and modified membrane using the four-point method: two working electrodes (a stainless steel cathode and a mixed-metal-oxide-coated titanium anode) were used to apply the current, while the voltage drop across the membrane was measured using two calomel reference electrodes (ProSense B.V., QM712X). The reference electrodes were extended to a point as close to the membrane surface as possible using Haber–Luggin capillaries. During the experiments the temperature was maintained at 25 °C, and the applied current density was increased stepwise, every 30 s, to allow the membrane reach a steady state.

EIS measurements were carried out to get further insight about the influence of the interface layers of the membranes. These experiments were conducted using IviumStat XR, a potentiostat/galvanostat with frequency response analyzer (Ivium Technologies, the Netherlands). Similar to the DC current–voltage measurements, a four-point system was applied to measure the impedance of the membranes. All the impedance measurements were performed with an AC signal of 10 mA amplitude in the frequency range of 0.03 Hz–1 kHz. The complex nonlinear least-squares fitting of the impedance data was performed with the Zview 3.0 software package.

EIS results are generally represented by plotting the imaginary part of the impedance against its real part, which is known as the Nyquist plot. Then, to understand impedance spectra, the experimental results obtained with an electrochemical cell can be fitted to an equivalent electrical circuit (EEC). EECs are the result of the combination of different electrical elements (resistance, capacitors, etc.) connected in a logical order to allow a coherent interpretation of the mass transfer processes occurring in the system. Consequently, the contribution of each mass transfer process to the behavior of the membranes, which are simultaneous in time but predominate at different frequency ranges, can be elucidated from the parameters associated with their analogous electric elements in the EEC.

2.5. Permselectivity Measurements. The membranes were tested in galvanostatic mode under the application of a current density of 15 mA/cm^2, which is in the underlimiting range for all the studied membranes. These experiments were conducted using the same six-compartment module (Figure 2) and for the same mixture of NaCl and $CaCl_2$ in both compartments next to the membrane, to avoid any influence of concentration gradients between both sides of the membrane. The experiments lasted for 6 h, and samples were drawn every hour, from both compartments adjacent to the membrane being tested. Na^+ and Ca^{2+} concentrations were determined by HPLC (Agilent 1100 Series). This technique has ~2% error limit.

The permselectivity of the membranes between sodium and calcium ions (P_{Ca}^{Na}) was calculated according to an equation adapted from the paper of Sata et al.[26]

$$P_{Ca}^{Na} = \frac{t_{Na^+}/t_{Ca^{2+}}}{C_{Na^+}/C_{Ca^{2+}}} = \frac{J_{Na^+}\cdot C_{Ca^{2+}}}{J_{Ca^{2+}}\cdot C_{Na^+}} \quad (1)$$

$$t_{Na^+} = \frac{J_{Na^+}}{\sum J_i} \quad (2)$$

$$t_{Ca^{2+}} = \frac{J_{Ca^{2+}}}{\sum J_i} \quad (3)$$

where C is the concentration of the ions on the diluate side of the membranes expressed in mol/L, J is the flux of the ions through the membrane expressed in mol/m^2·s, and t is the transport number of the ions through the membrane. The flux of ions was obtained from the change in concentration of the ions on the diluate side according to

$$J_{Na^+} = \frac{V\cdot\frac{dC_{Na^+}}{dt}}{A_m} \quad (4)$$

$$J_{Ca^{2+}} = \frac{V\cdot\frac{dC_{Ca^{2+}}}{dt}}{A_m} \quad (5)$$

dx.doi.org/10.1021/am4048317 | ACS Appl. Mater. Interfaces 2014, 6, 1843–1854

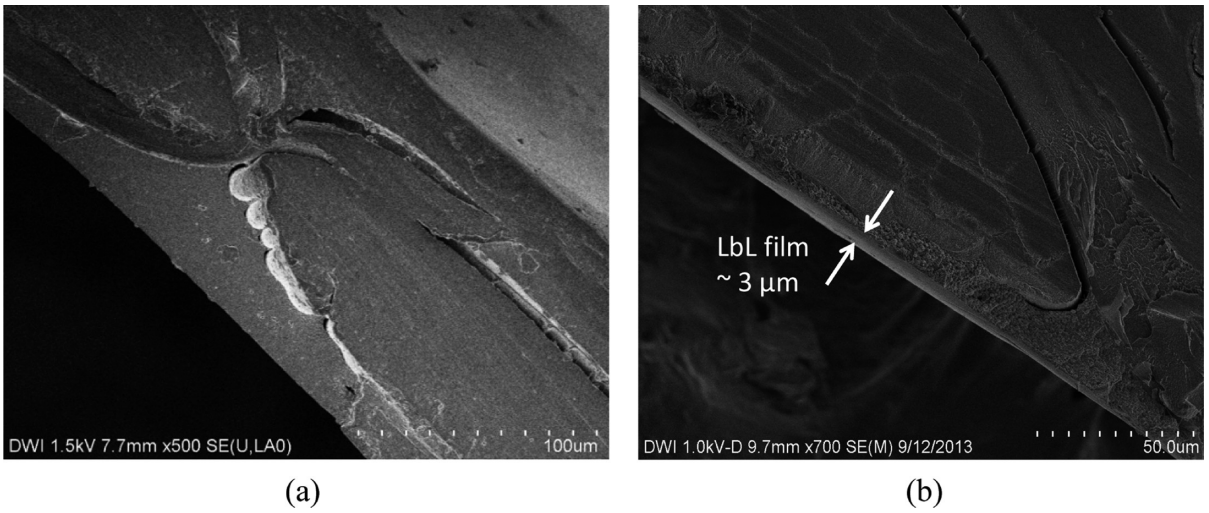

Figure 3. Cross-sectional FE-SEM micrographs obtained for (a) an unmodified CMX membrane and (b) a CMX membrane modified with 10.5 bilayers of PEI/PSS (both polyelectrolytes prepared in 0.5 M NaCl solution).

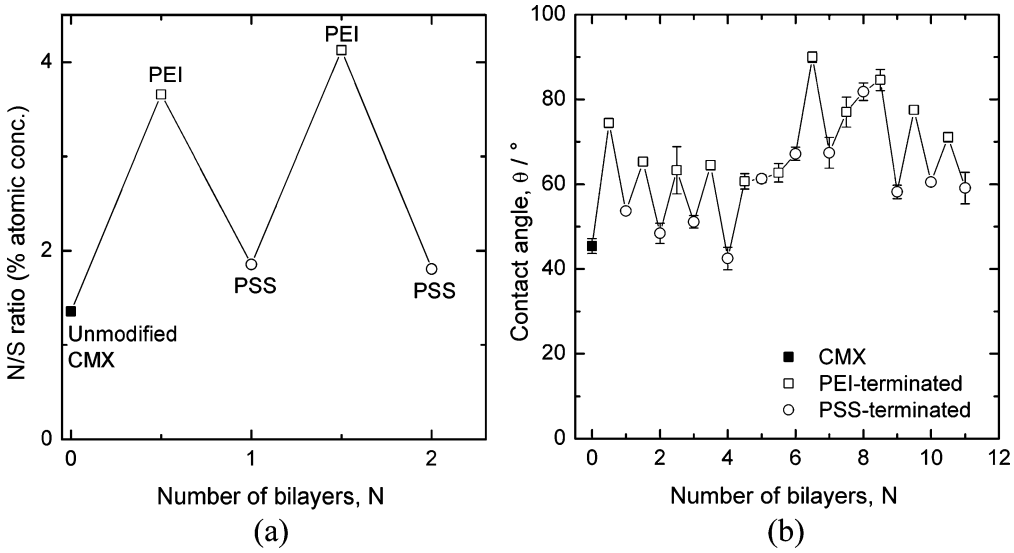

Figure 4. Surface characterization of the modified membranes: (a) N/S ratio and (b) water contact angle values as a function of the number of bilayers.

where V is the volume of the treated batch of the electrolyte, which was 1 L, and A_m is the active area of the membranes, which was 10.5 cm^2.

Furthermore, the specific energy consumption in the membrane region per mole of transported Na^+ ions (E_m) was calculated according to the relation

$$E_m = \frac{\int U_m \cdot I dt}{(C_o - C_t)V} \quad (6)$$

where I is the applied current; U_m is the voltage drop across the membrane measured by the reference electrodes; C_o and C_t are the concentrations of Na^+ ions initially and at a specific time t, respectively.

3. RESULTS AND DISCUSSION

3.1. Surface Characterization of the Modified Membranes. The effect of the deposition of LbL assemblies on the surface properties of the modified membranes was assessed by means of various techniques. For a high number of deposited layers, FE-SEM allows the identification of the LbL films coated on top of the membranes. Figures 3(a) and 3(b) show the cross-sectional images of an unmodified and a modified CMX membrane, respectively. In both micrographs, the structure of the CMX membrane composed of the membrane matrix and the reinforcing fibers can be seen. In the case of the modified membrane the deposited LbL film (10.5 bilayers) can be clearly distinguished from the membrane substrate. Normally, for membrane samples that are coated with few polyelectrolyte layers, the LbL film is very thin and cannot be clearly detected in the FE-SEM images.

In the case of a low number of deposited layers, XPS is a useful tool to monitor the deposition of the LbL films on top of the substrate membrane since the functional groups of PEI and PSS are composed of different elements. Figure 4(a) shows the evolution of the ratio of nitrogen to sulfur (N/S) atomic concentration for the first two bilayers. The alternating trend of the N/S ratio with the number of deposited bilayers reveals an increase in the presence of nitrogen when PEI is the last layer adsorbed and an increase in the concentration of sulfur when the last adsorption step is conducted with PSS. The increase in the atomic concentration of nitrogen is associated with the

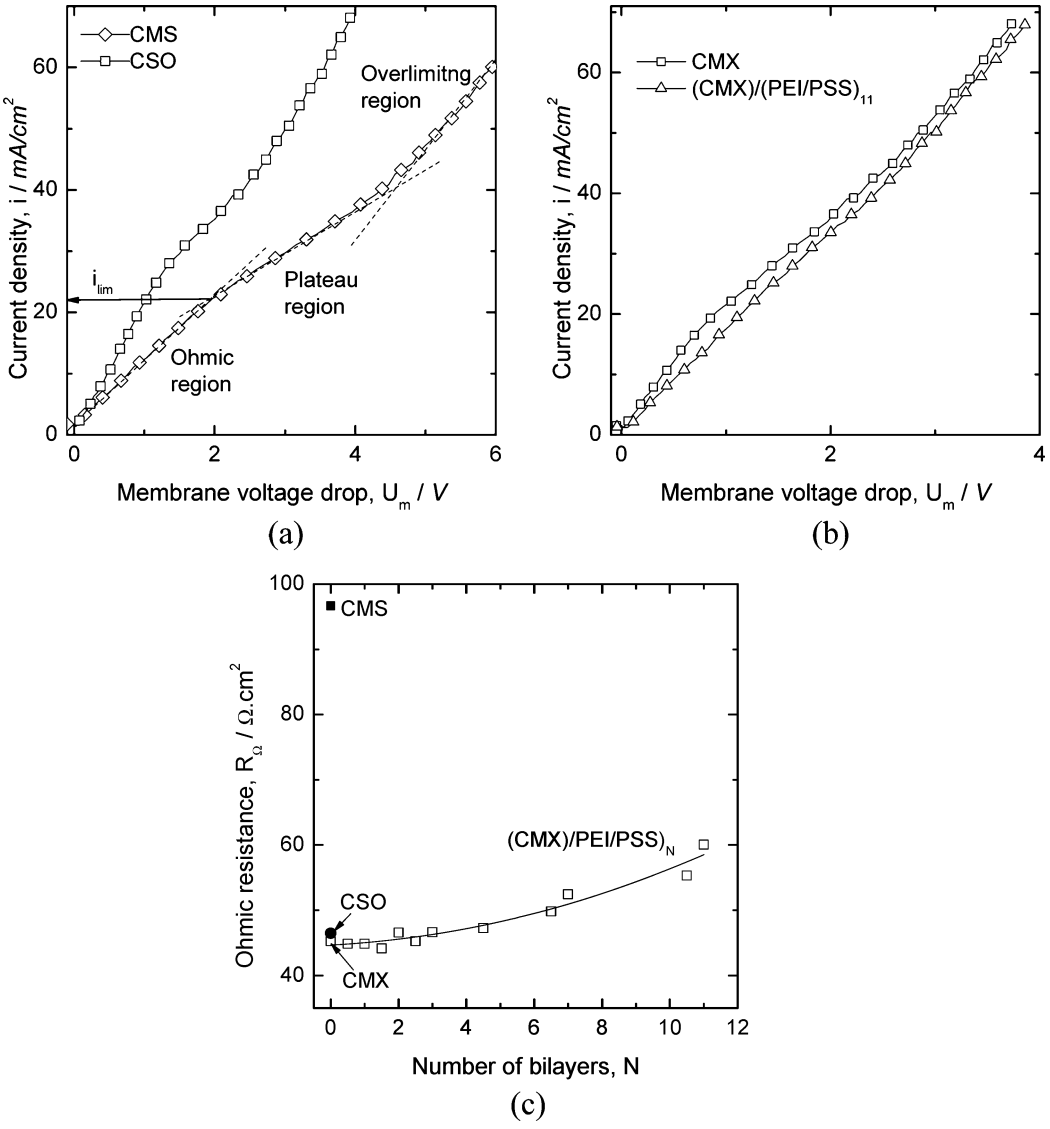

Figure 5. Current–voltage curves obtained with mixtures of 0.05 M NaCl and 0.05 M $CaCl_2$ for (a) the two monovalent-ion-permselective membranes CMS and CSO and (b) unmodified CMX membrane and one modified with 11 bilayers of PEI/PSS, with the scatter of the overlimiting region of the graphs smoothed. (c) Dependence of the R_Ω values of the membrane/electrolyte system as a function of the number of bilayers.

amine groups present in the PEI top layer, whereas the sulfonic groups of PSS are responsible for the increase in the sulfur content.

In addition to the FE-SEM images and the XPS analysis, measurement of the contact angle provides an additional indication of the changes brought about on the membrane surface as a consequence of the polyelectrolyte deposition. The contact angle measurements as a function of the number of bilayers deposited are shown in Figure 4(b). In general, when the top layer is PEI the membrane hydrophobicity increases, and when it is PSS the membrane surface becomes more hydrophilic. This alternating trend confirms, as observed in the XPS analysis, the effective sequential deposition of both polyelectrolytes. It has to also be noted that contact angle values increase somewhat for the samples modified with more than five bilayers. This behavior could be due to the increase in the thickness of the LbL assembly with increasing number of adsorption steps. For the first adsorption steps, there may exist some coating defects with areas where the membrane substrate is not covered by the polyelectrolyte chains. Hence, during the contact angle measurement of these membranes, part of the water droplets may reach the base membrane, thus resulting in contact angles closer to that of the unmodified membrane (45.4°). However, as the number of bilayers increases and the membrane surface gets completely covered, the contact angle is mostly dependent on the properties of the LbL coating. In the results obtained by other authors a change in the trend of the contact angle measurements from approximately more than five bilayers was also reported.[13,25]

3.2. Electrochemical Characterization of the Modified Membranes. *Current–Voltage Curves.* Polarization current–voltage curves are a necessary tool to characterize the behavior of ion exchange membranes over a wide range of currents. Typical current–voltage curves obtained for monopolar ion exchange membranes display three different membrane behaviors depending on the applied current. At low current densities, the current is directly proportional to the membrane voltage drop, and therefore, the transport through the membrane can be described by a quasi-ohmic behavior. As the current is further increased and the limiting current density

dx.doi.org/10.1021/am4048317 | ACS Appl. Mater. Interfaces 2014, 6, 1843–1854

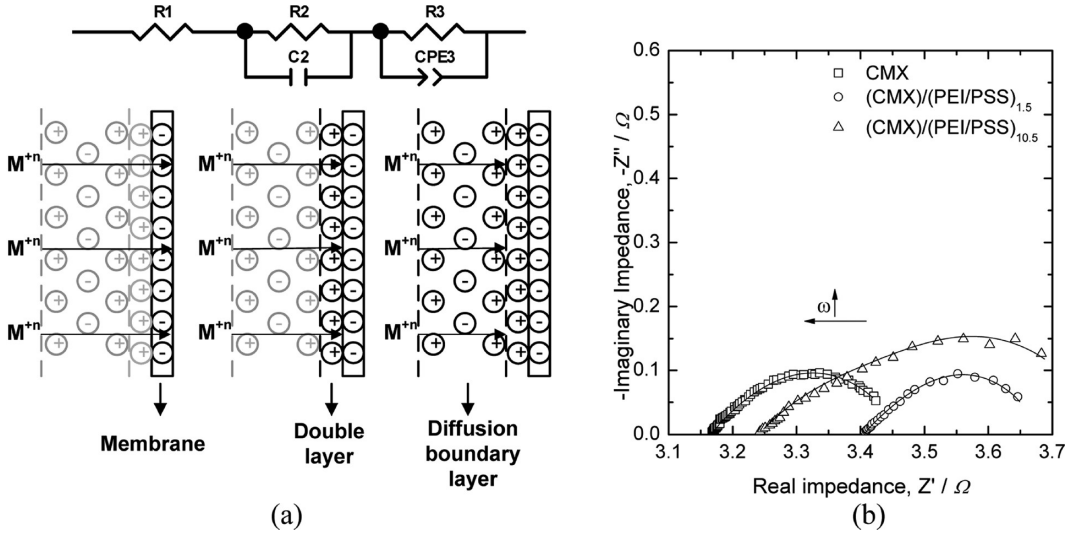

Figure 6. (a) EEC for the cation exchange membrane with solution used in this study and schematic diagram of the phenomena associated with each component of the circuit. At very high frequencies the impedance shows only the ohmic resistance due to the membrane and the solution; at medium frequencies the heterogeneous transport layer originates the capacitive behavior; and at low frequencies the transport of electroactive species through the solution layers is modeled with a constant phase element. (b) Nyquist plot representation of the impedance responses obtained for the unmodified CMX membrane and other modified membranes.

(i_{lim}) for the membrane/electrolyte system is reached, the concentration of counterions in the diluate side of the ion exchange membrane strongly diminishes due to the more rapid transport through the membrane as compared to the diffusive supply out of the bulk liquid through the diffusion boundary layer. As a consequence, the resistance of the membrane system increases, and a plateau is formed in the curve. The increase in resistance stems from the continuous ion depletion of the diffusion boundary layer. The third part of the curves, known as the overlimiting region, appears at an advanced stage of concentration polarization. The membrane voltage drop reaches a certain threshold at which multiple phenomena occur that can destabilize the boundary layer:[27−29] supply of counterions to the membrane surface is enhanced, and current density values increase again with the membrane voltage drop. The plateau length and the onset of the overlimiting current are not well understood yet but are not the object of the current study.

Figures 5(a) and 5(b) show some of the curves obtained for the modified and unmodified commercial membranes. The curves exhibit the three characteristic regions described above, which are indicated for the CMS membrane in Figure 5(a). Different aspects of the ionic transport through ion-conducting membranes can be evaluated from the curves. The ohmic resistance (R_Ω) can be obtained from the inverse of the slope of the first ohmic part of the curves. An increase in the ohmic resistance of the modified membranes would be expected as the thickness of the LbL film increases with the number of deposited bilayers.

The values of R_Ω are presented in Figure 5(c) for the commercial (CMX, CMS, and CSO) and various modified membranes ($(CMX)/(PEI/PSS)_N$). Among the commercial membranes, the lowest R_Ω value was calculated for the unmodified CMX membrane (45.25 $\Omega\cdot cm^2$). The resistance of the monovalent-ion-permselective CSO membrane is similar to that of CMX, whereas the highest resistance is that of the monovalent-ion-permselective CMS membrane. The increased R_Ω value obtained for CMS could not be ascribed only to the thin cationic layer deposited on its surface. Tuan et al. reported that the CMS membrane is characterized by having a higher degree of cross-linking in addition to the thin cationic layer deposited on its surface.[30] The enhanced cross-linking is another factor imparting monovalent ion permselectivity properties to this membrane. Therefore, the mobility of larger cations through its structure may be diminished due to ion-size impediments, which are also responsible for the high electrical resistance observed for this membrane.

In the case of the modified membranes, R_Ω values show a very slight increase with the number of adsorbed bilayers. As expected, among the modified membranes, those with the highest number of bilayers (10.5 and 11 bilayers) present the largest R_Ω values. Such an increase with respect to the unmodified CMX membranes starts to be noticeable for a number of bilayers higher than 6. These results could be related to the total coverage of the substrate membrane achieved from a certain number of bilayers in the LbL film. Moreover, it has to be noted that the highest R_Ω value calculated for the modified membranes (60.06 $\Omega\cdot cm^2$ for $((CMX)/(PEI/PSS)_{11})$ is even lower than that of the monovalent-ion-permselective CMS membrane. As stated previously, the slight increase in the membrane resistance with the number of polyelectrolyte layers can be considered as an additional proof of the successful deposition of LbL assemblies on the cation exchange membranes.

With regard to the limiting current density, as can be seen from Figure 5(a), the i_{lim} values lie approximately around 20 mA/cm^2 for all the investigated membranes. The slight variation in the i_{lim} values and the less well-defined transition region could be explained as a consequence of the compensation between the effects of the increased hydrophobicity and the conducting heterogeneity of the LbL assemblies.[31,32]

Impedance Measurements. In addition to the changes promoted by the LbL modification of the membranes on the current−voltage characteristics, the main contribution of the LbL films to the membrane permselectivity may be caused by

Table 2. Best-Fit Estimates of the EEC Parameters Obtained from the Impedance Measurements for the Unmodified and Modified CMX Membranes

number of (PEI/PSS) bilayers	0	0.5	1	1.5	6.5	7	10.5
R_1 (Ω)	3.17 ± 0.00	3.23 ± 0.00	3.20 ± 0.00	3.41 ± 0.00	3.50 ± 0.00	3.37 ± 0.00	3.27 ± 0.00
R_2 (Ω)	0.018 ± 0.001	0.021 ± 0.000	0.031 ± 0.002	0.020 ± 0.000	0.049 ± 0.002	0.113 ± 0.003	0.111 ± 0.002
R_3 (Ω)	0.273 ± 0.003	0.298 ± 0.002	0.221 ± 0.003	0.256 ± 0.001	0.310 ± 0.004	0.345 ± 0.004	0.370 ± 0.005
C_2 (F)	14.14 ± 0.91	8.22 ± 0.59	10.19 ± 1.50	9.73 ± 0.59	6.34 ± 0.71	5.35 ± 0.29	4.89 ± 0.22
CPE_3–Q ($S \cdot s^n$)	22.74 ± 0.55	22.74	22.74	22.74	22.74	22.74	22.74
CPE_3–n (−)	0.77 ± 0.01	0.77 ± 0.00	0.80 ± 0.01	0.79 ± 0.00	0.85 ± 0.00	0.84 ± 0.01	0.87 ± 0.01
χ^2	7.55×10^{-5}	1.28×10^{-4}	2.77×10^{-4}	8.12×10^{-5}	2.27×10^{-4}	1.70×10^{-4}	2.41×10^{-4}

the change in the attractive/repulsive forces existing between the surface of the modified membranes and the electrolyte counterions. In this context, EIS is an electrochemical technique that potentially provides information about the charging properties of interfaces. Particularly, a recent work shows that EIS can distinguish among the diffusion boundary layer resistance, the double-layer resistance, and the transfer resistance from the liquid into and through the membrane phase.[33]

The EEC used to fit the EIS of the different membranes thus considers the combination in series of the contributions of the three different layers to the mass transfer resistance: the combined ohmic resistance of membrane and solution, the double layer formed at the membrane/solution interface, and the diffusion boundary layers.[33−36] The EEC and the schematic representation of the three transport layers considered are shown in Figure 6(a). This circuit has already been used in previous studies to investigate the behavior of ion exchange membranes.[33,35,37]

At the high frequency range, the system behavior is purely resistive, which is defined by the combined ohmic resistance of the solution and the membrane (R_1).

As the frequency decreases, a phase shift between the voltage and current signals is usually observed. This response corresponds to a capacitive behavior modeled in the EEC with a resistor (R_2) and a capacitor (C_2) connected in parallel. The R_2–C_2 combination represents the mass transfer occurring at the electrical double layer formed at the membrane/electrolyte interface, where the current is divided into its faradaic component and another part used to charge the double layer. Finally, when the range of low frequencies is reached, the transport in the solution layers becomes predominant in the EIS response. This behavior can be adjusted to the parallel combination of a resistance (R_3) and a constant phase element (CPE_3). The constant phase element is a nonintuitive element, which can represent all types of impedance behavior and takes into account nonhomogeneities in the material or nonideal behaviors.[38]

An example of the Nyquist plots obtained with the unmodified CMX and some modified CMX membranes is presented in Figure 6(b). The resistance R_1 is calculated from the intercept at high frequencies with the x-axis (no imaginary part). At decreasing frequencies two overlapped semicircles corresponding to the R_2–C_2 and R_3–CPE_3 elements appear in the diagram. The fittings are represented in solid lines in Figure 6(b), and the best-fit estimates of the EEC parameters are tabulated with the chi-square (χ^2) values of the model fitting in Table 2. Since the operating conditions during the experiments were the same (such as the volume flow rate or the 0 DC current), we assume the properties of the solution layers to be approximately constant for all the membranes. Accordingly, the values of the constant phase element (CPE_3–Q) were fixed to the value obtained with the unmodified CMX membrane to get better estimations for the rest of the parameters of the modified membranes.

From the fitting results, the parameter which is most influenced by the LbL coatings is the capacitance of the double layer (C_2). C_2 values exhibit an abrupt decrease for the first adsorbed layer of PEI, which may be associated with a charge reversal of the membrane surface. Then, an alternating trend is observed for the first polyelectrolyte bilayers, where the values of C_2 increase when the last adsorbed polyelectrolyte is PSS and decrease when the last adsorbed polyelectrolyte is PEI. As an analogy, Sow et al. reported a decreasing trend in the capacitance of the double layer of ion exchange membrane systems with increasing temperature, which was attributed to a decrease in the Donnan potential.[38] In the present case, the decreasing C_2 values could stem from the decrease in the proportion of negative fixed charges on the membrane surface as the number of bilayers is increased and the positively charged layers of the hyperbranched PEI overlap. As the number of polyelectrolyte multilayers increases, the increase in the proportion of positive charges at the surface of the membrane would reduce the Donnan potential, which is regarded in the literature as indicative for the reduction in the membrane permselectivity for counterions. However, in the present case, the decrease in the Donnan potential may be interpreted as a consequence of the enhanced repulsive forces in the LbL film toward multicharged counterions, thus resulting in a decrease of the charging properties of the membrane/solution interface. In addition, the decrease of capacitance has also been attributed to the thickening of layers deposited on the surface of ion exchange membranes.[39]

With regard to the other parameters, only slight changes can be observed. Minor variations in the values of R_1 are observed with the increase of the number of bilayers, thus confirming the moderate influence of the LbL films on the electrical resistance observed from the current−voltage curves. However, it is important to note that these slight variations observed in the R_1, R_2, and R_3 values for the different membranes may also be influenced by measurement inaccuracies, as it is usually reported for the through-plane measured impedance of ion exchange membranes.[40]

Finally, it should be noted that the parameter CPE_3–n takes values close to 0.8. Park et al. reported values of the CPE_3–n between 0.7 and 0.8, which were attributed in that case to an insignificant development of diffusion boundary layers (typically associated with n values of 0.5) and the predominant role of convective transport.[35]

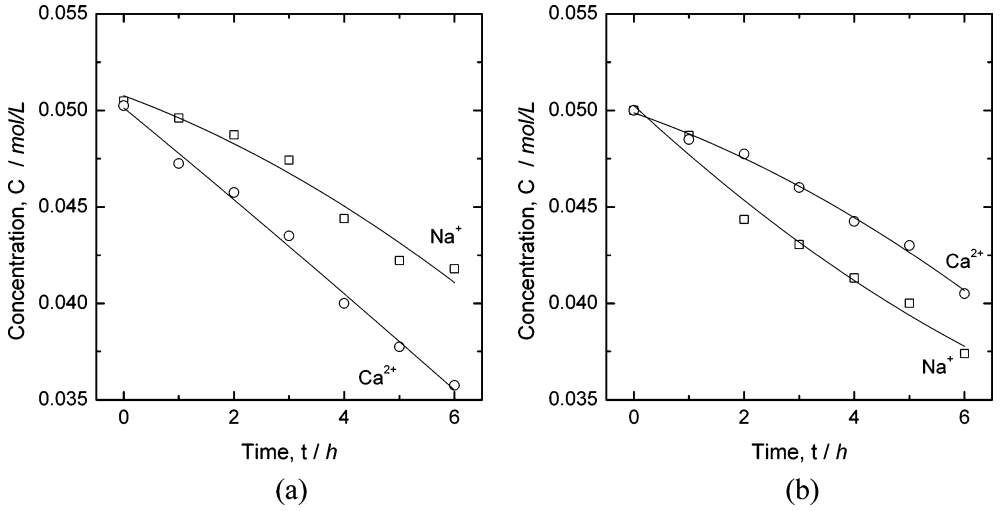

Figure 7. Evolution of Ca^{2+} and Na^{+} ion concentrations in the diluate compartment, with the (a) unmodified CMX membrane and (b) CMX modified with LbL film of 11 bilayers. Values corrected for very slight differences in the initial concentrations.

3.3. Evaluation of Monovalent Ion Permselectivity.

The monovalent ion permselectivity of the modified membranes was evaluated by measuring the evolution of Ca^{2+} relative to Na^{+} ion concentrations in the diluate compartment. Typical concentration profiles for the unmodified CMX membrane and one modified membrane (with 11 bilayers of PEI/PSS) are shown in Figure 7. The performance of the modified membranes was compared against commercial benchmarks, i.e., the commercially available monovalent-ion-permselective membranes: Neosepta CMS (Astom, Japan) and Selemion CSO (AGC, Japan). The complete results of Ca^{2+}/Na^{+} flux, monovalent ion permselectivity, and specific energy consumption of all the studied membranes are presented in Table 3 and Table 4.

Table 3. Ca^{2+}/Na^{+} Flux, Monovalent Ion Permselectivity, and Specific Energy Consumption Values of the Commercial Membranes

	membrane		
	CMX	CMS	CSO
$J(Ca^{2+})$ (10^{-4} mol/m^2·s)	6.45	4.18	3.52
$J(Na^{+})$ (10^{-4} mol/m^2·s)	4.03	5.31	6.08
P_{Ca}^{Na}	0.64	1.23	1.72
$E_{s,m}$ (Wh/mol Na^{+})	49.96	80.73	42.81

Monovalent Ion Permselectivity of Commercial Membranes. The measured flux of Ca^{2+} and Na^{+} ions and the resulting permselectivities between calcium and sodium ions (P_{Ca}^{Na}) of the commercial membranes are presented in Table 3. The results show that for the CMX membrane the migration of divalent ions was higher than the monovalent ones, which leads to P_{Ca}^{Na} values lower than one.

The results shown in Table 3 also reveal that the commercial monovalent-ion-permselective membranes CSO and CMS present higher J_{Na+} values than J_{Ca2+}, as expected. The monovalent ion permselectivity in CSO is probably imparted due to a thin positively charged coating on the surface of the membrane, which repels multivalent cations. On the CMS membrane the monovalent ion permselectivity is partly related to an active layer on the surface, and it could also be due to the possible presence of a high degree of cross-linking on the membrane matrix (styrene-divinylbenzene).[41]

The voltage drop across the membranes was also measured during the permselectivity experiments and was then used to calculate the specific energy consumption of the membrane system per mole of transported Na^{+} ions. While the standard CMX membrane requires ~50 Wh/mol Na^{+}, CMS requires significantly higher specific energy of ~80 Wh/mol Na^{+}. On the other hand, it is noteworthy that the CSO membrane exhibits rather low energy consumption, about half that of CMS. This striking difference in the energy consumption could be due to the fact that the CMS membrane possesses a dense membrane matrix.

Monovalent Ion Permselectivity of the Modified Membranes: Effect of Number of Bilayers. The measured permselectivities between calcium and sodium ions (P_{Ca}^{Na}) of the modified membranes are depicted in Figure 8, showing the effect of the number of bilayers. The figure reveals that single layer formation of PEI (i.e., (CMX)/$(PEI/PSS)_{0.5}$) has not improved the monovalent ion permselectivity to the level of the commercial monovalent-ion-permselective membranes. The

Table 4. Ca^{2+}/Na^{+} Flux, Monovalent Ion Permselectivity, and the Specific Energy Consumption Values of the LbL-Modified Membranes: Effect of Number of Bilayers

	number of PEI/PSS bilayers										
	0	0.5	1	1.5	2	2.5	3	6.5	7	10.5	11
$J(Ca^{2+})$ (10^{-4} mol/m^2·s)	6.45	4.56	5.75	3.77	6.02	4.57	4.42	4.16	3.51	4.40	4.06
$J(Na^{+})$ (10^{-4} mol/m^2·s)	4.03	4.99	4.35	4.37	4.88	5.75	4.94	5.34	3.90	6.01	5.51
P_{Ca}^{Na}	0.64	1.09	0.76	1.15	0.83	1.20	1.08	1.24	1.17	1.35	1.31
$E_{s,m}$ (Wh/mol Na^{+})	49.96	41.55	48.52	48.17	41.88	54.96	53.87	40.37	56.57	48.60	53.76

dx.doi.org/10.1021/am4048317 | ACS Appl. Mater. Interfaces 2014, 6, 1843−1854

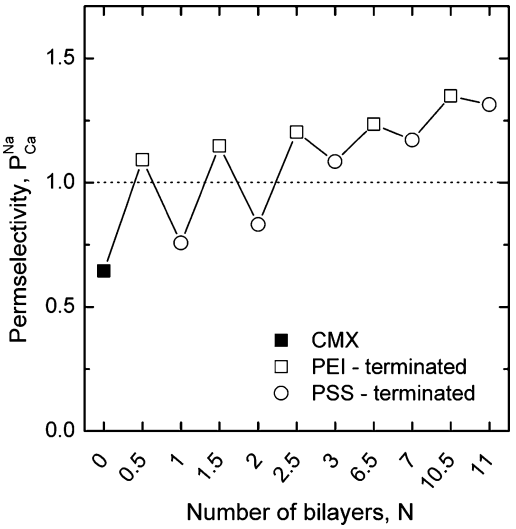

Figure 8. Measured permselectivities between sodium and calcium ions of the modified CMX membranes as a function of the number of $(PEI/PSS)_N$ bilayers.

strategy of single layer formation of PEI on the surface of cation exchange membranes was long investigated by Sata and Mizutani.[42] It was shown in their work that 1 g/L of PEI was optimal and a further increase in the polyelectrolyte concentration did not enhance the permselectivity. Accordingly, we have adopted this concentration for our LbL assembly. Unlike coating of a single layer of PEI, with the LbL approach, increased concentration of positive charges can be achieved on the surface of cation exchange membranes. Furthermore, the structures formed by LbL assembly are robust, as a result of the strong electrostatic bonding within the LbL layers.

Figure 8 in addition reveals that the permselectivity of the membranes modified by polyelectrolyte multilayers shows different behavior depending on the number of deposited bilayers. The typical "odd−even" effect of the coated membranes can also be observed, whereby the permselectivity of the modified membrane is improved, when the LbL coating is terminated with a layer of PEI. This odd−even effect is stronger at lower number of deposited bilayers and decreases with the number of deposited bilayers, eventually almost fading away at 10.5 and 11 bilayers. With respect to the PEI-terminated layers, as mentioned before, with deposition of the first PEI layer, a steep increase in the permselectivity can be observed in comparison to the unmodified CMX membrane. Then the P_{Ca}^{Na} values increase progressively with the number of deposited bilayers. At 6.5 bilayers already, a permselectivity (1.24) comparable to that of the CMS membrane was achieved.

The enhanced repulsion of divalent ions by the modified membranes is most likely the result of two effects: an increase of positive charges on the surface of cation exchange membranes as well as increased hydrophobicity on the same. The former effect increases with increasing number of bilayers due to the multibipolar structure of the polyelectrolyte multilayers. The multibipolar structure (shown schematically in Figure 9) enables fractionation of mono- and divalent ions because of a more pronounced Donnan exclusion towards the divalent ions, as discussed by Krasemann and Tieke.[43] In other words, the multivalent cations would experience a higher electrostatic repulsion by the positively charged layers of PEI

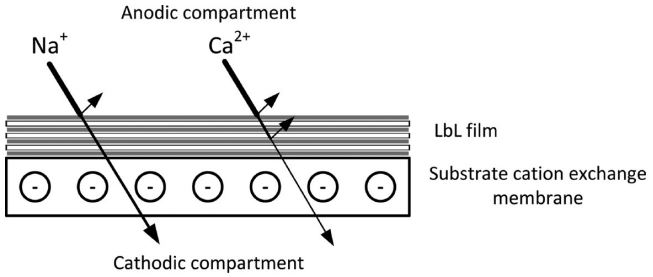

Figure 9. Schematic representation of rejection of cations on the multibipolar structure of the LbL layers atop of a cation exchange membrane (adapted from refs 43 and 44). Multivalent cations would experience higher Donnan exclusion successively, at the positive parts of the LbL film.

deposited in the LbL film. Under the application of a constant current, the weaker repulsions of the LbL film toward monovalent ions would favor the fact that these ions can permeate easier through the membrane than multivalent ions.

The second effect is the concomitant hydrophobization of the membrane surface. This behavior can be correlated with the contact angle measurements (Figure 4(b)), where at high number of bilayers the contact angle of the membranes increased in comparison to the contact angle of the unmodified membrane. This behavior, as noted above, is explained to be the result of a more or less complete coverage of the substrate membrane by the polyelectrolyte layers. Therefore, the contact angles tend towards the real values of the PEI/PSS without the effect of the underlying substrate.

In electrodialysis, ions migrate with their hydration shells. To pass the solution/membrane interface, ions need to overcome an energy barrier, imposed by the requirement of their partial dehydration. Hence, the effect of this barrier is likely to be higher with monovalent-ion-permselective membranes or hydrophobized membrane surfaces.[45−47] Indeed, in the investigation of Firdaous et al. with monovalent ion permselective membranes,[46] ionic flux of chloride salts of three metal ions decreased in the sequence $J_{Na+} > J_{Ca2+} > J_{Mg2+}$. They followed the order of an increase in their hydration energy, as shown in Table 5.[48,49] This observation was attributed to the above-discussed effect.

Table 5. Physico-Chemical Properties of Sodium, Calcium, and Magnesium Ions [Taken from References 48 and 49]

ion	ionic radius (nm)	hydrated-ionic radius (nm)	Gibb's hydration energy (kJ/mol)
Na^+	0.102	0.218	365
Ca^{2+}	0.100	0.271	1505
Mg^{2+}	0.072	0.299	1830

Referring to the specific energy consumption data of the coated membranes in Table 4, no specific trend can be observed. The values vary between approximately 40 and 60 Wh/mol Na^+ ions. The membrane with 6.5 bilayers coating had the lowest specific energy consumption for the passage of 1 mol of Na^+ ions. For membranes coated with more than 6.5 bilayers, despite an improvement in the permselectivity, the specific energy consumption increases with the number of bilayers, due to higher electric resistance of the membranes. Hence, in terms of ease of coating, the achieved permselectivity, and the specific energy consumption, the membrane with 6.5 bilayers seems optimal. This of course depends on the target

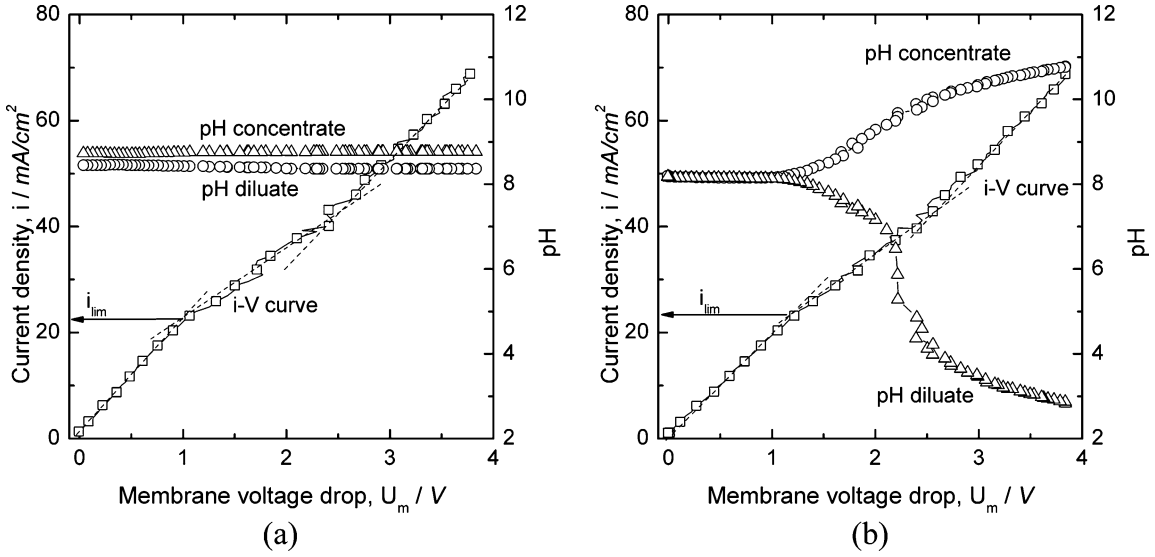

Figure 10. Polarization curves along with pH measurements for (a) unmodified CMX and the (b) modified CMX membrane (with 10.5 bilayers of PEI/PSS).

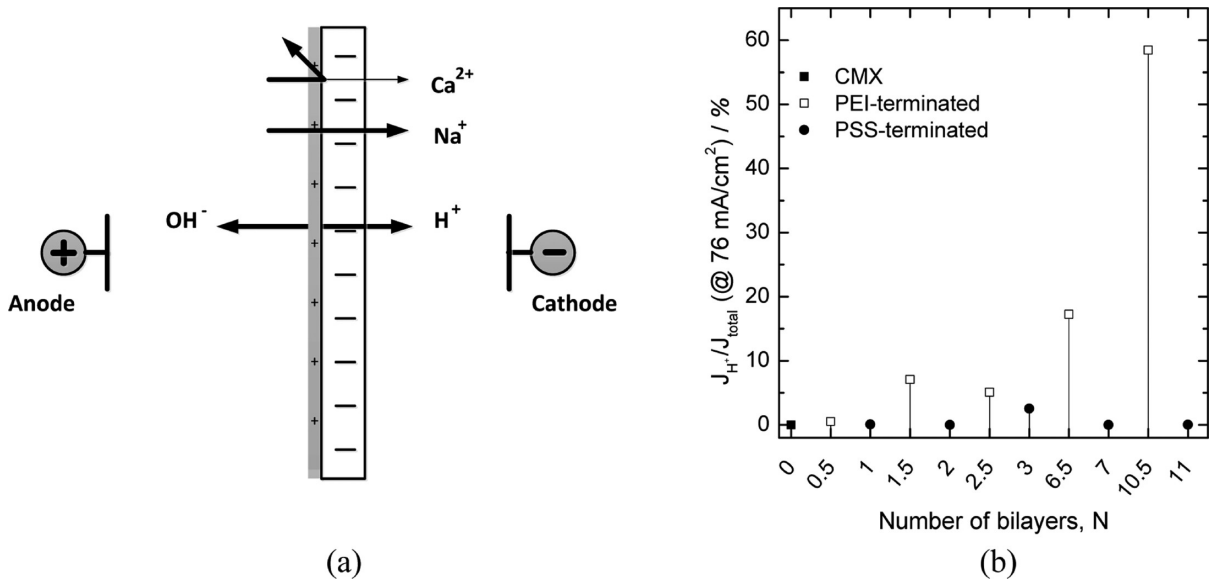

Figure 11. (a) Schematic of competitive ion transport through the modified membranes in the overlimiting current regime in a state of water splitting. (b) Ratio of flux of protons to the total ion flux as a function of deposited number of bilayers.

industrial applications; i.e., the value of the metal ions to be recovered and the cost related to the electrical energy consumption have to be compromised. On the other hand, for the commercial membrane CMS, the monovalent ion permselectivity is achieved at the expense of energy consumption; CMS requires twice as much specific energy demand of the membrane coated with 6.5 bilayers, for the passage of 1 mol of Na^+ ions.

The above effect of the number of bilayers on the permselectivity was manisfested for constant current density experiments in the ohmic region. Detailed data analysis of the polarization curves in the overlimiting current region reveals another remarkable effect. The polarization curves of the unmodified CMX and one modified CMX membrane (with 10.5 bilayers of PEI/PSS), with the simultaneously recorded pHs, are shown in Figure 10(a) and (b), respectively. For the unmodified CMX membrane there is hardly any change in pH. Conversely, for some of the modified membranes (as exemplified in Figure 10(b)), there is a strong variation of pH caused by water splitting, starting from the limiting current density.

The water splitting could originate from the catalytic activity of the LbL layers on the surface of cation exchange membranes, thus acting as quasibipolar membranes.[23] However, unlike bipolar membranes which reject all kinds of ions, these membranes still allow the passage of cations, when overlimiting currents are applied as shown schematically in Figure 11(a). A summary of the analysis of the water splitting flux is depicted in Figure 11(b), which shows the ratio of the flux of protons across the cation exchange membranes to the total ion flux (i.e., Na^+, Ca^{2+}, and H^+ ions) at a current density of 76 mA/cm^2. The graph clearly exhibits that the water splitting depends strongly on the nature of the last layer deposited. Water splitting is absent in those membranes terminated with PSS in

dx.doi.org/10.1021/am4048317 | ACS Appl. Mater. Interfaces 2014, 6, 1843−1854

the range up to 11 bilayers, whereas the water splitting rate increases with the number of PEI-terminated layers. For instance, for the membrane with 10.5 bilayers of polyelectrolytes, the flux of protons is ~60% of the total ion flux at a current density of 76 mA/cm^2. There are some applications where ion permselectivity is needed, and at the same time the pH should be regulated.[50] Our LbL-modified ion exchange membranes could be a key to such symbiosis.

In previous studies with pressure-driven membrane processes, it was shown that permselectivity of the modified membranes depends strongly on the selected polyelectrolyte pairs used to modify the membranes as well as on the LbL deposition parameters.[43,51] To investigate the effect of LbL deposition parameters of the polyelectrolyte pairs, several LbL parameters were varied, with optimal number of bilayers of this series, i.e., 6.5 bilayers. The membranes were coated, with the addition of salt and reversed molecular weight asymmetry of the PEI/PSS polyelectrolyte pairs. To prepare the membrane with addition of salt, both polyelectrolytes were dissolved in 0.5 M NaCl. The multilayers with the reversed MW asymmetry were formed from 25 000 g/mol PEI and 1 000 000 g/mol PSS. Furthermore, PAH (pH = 3.0), along with PSS, was used instead of the PEI/PSS pair. The effect of the above variations was minimal on the permselectivity between Na^+ and Ca^{2+} ions. Nonetheless, there was a significant difference in the specific energy consumption values. The results of these variations on the permselectivity and the specific energy consumption can be found in the Supporting Information.

It is worth mentioning that the achieved monovalent ion permselectivity is also a strong function of the operating parameters, like stack design, feed concentrations, and current density.[9,52] In industrial stacks, cell configurations and hydrodynamic conditions could be optimized to achieve lower P_{Ca}^{Na} values. These considerations, however, are clearly beyond the scope of this paper.

4. CONCLUSIONS

In conclusion, competitive ion transport through LbL-modified cation exchange membranes was studied, with the main objective of inducing monovalent ion permselectivity on the membranes. It was demonstrated that the LbL assembly was successfully implemented on cation exchange membranes, without any pretreatment of the membranes as confirmed with FE-SEM, contact angle, and XPS measurements. Coating of the LbL layers caused only moderate variation of the ohmic resistance of the membrane systems. Nonetheless, the LbL layers had a substantial influence on the monovalent ion permselectivity of the membranes. A typical "odd−even" effect was present in the permselectivity, which was more prominent in the lower number of bilayers. As expected, the permselectivity was improved when the coating was terminated with PEI (positive) layers. Permselectivity comparable to that of a commercial monovalent-ion-permselective membrane was obtained with only six bilayers of polyelectrolytes, yet with significantly lower energy consumption per mole of transported Na^+ ions. The monovalent ion permselectivity was explained to be induced as a result of synergy of two effects: increased Donnan exclusion for divalent ions and hydrophobization of the surface of the membranes that accompanies their modification. Furthermore, the double-layer capacitance obtained from impedance measurements was shown to be a qualitative indication of the divalent ion repulsion of the membranes, when the membranes are characterized in a mixture of mono- and divalent salts.

Yet another major finding was observed with regard to the water splitting behavior of the modified membranes. At current densities higher than the limiting current density, there was a strong change in the electrolyte pH of some of the modified membranes, which was insignificant for the unmodified CMX membrane. The flux of protons across the modified membranes increased with the number of PEI-terminated bilayers, while it was nearly absent for the PSS-terminated bilayers, up to a range of 11 bilayers. There are applications in which ion permselectivity and pH regulation are needed at the same time; our LbL-modified ion exchange membranes could be a key to such symbiosis.

■ ASSOCIATED CONTENT

Supporting Information

Effect of varying the LbL deposition parameters on the monovalent ion permselectivity and the specific energy consumption of the modified CMX membranes. This material is available free of charge via the Internet at http://pubs.acs.org.

■ AUTHOR INFORMATION

Corresponding Author

*Tel.: +49 241 80 95470. E-mail: manuscripts.cvt@avt.rwth-aachen.de.

Author Contributions

⊥Both authors contributed equally to the paper.

Notes

The authors declare no competing financial interest.

■ ACKNOWLEDGMENTS

The authors from Germany acknowledge support through the German Research Foundation (DFG) grant − SFB 985 "Functional Microgels and Microgel Systems". M.C. Martí-Calatayud is grateful to the Universitat Politècnica de València for his postgraduate (Ref.: 2010-12) and visiting scientist grant (PAID-00-12). M. Wessling appreciates financial support from the Alexander-von-Humboldt Foundation.

■ REFERENCES

(1) Strathmann, H. *Desalination* **2010**, *264*, 268−288.
(2) Abels, C.; Carstensen, F.; Wessling, M. *J. Membr. Sci.* **2013**, *444*, 285−317.
(3) Saracco, G. *Chem. Eng. Sci.* **1997**, *52*, 3019−3031.
(4) Vallois, C.; Sistat, P.; Roualdès, S.; Pourcelly, G. *J. Membr. Sci.* **2003**, *216*, 13−25.
(5) Van der Bruggen, B.; Koninckx, A.; Vandecasteele, C. *Water Res.* **2004**, *38*, 1347−1353.
(6) Balster, J. H. Membrane module and process development for monopolar and bipolar membrane electrodialysis. *Ph.D. Thesis*, University of Twente, Enschede, 2006.
(7) Balster, J.; Krupenko, O.; Pünt, I.; Stamatialis, D. F.; Wessling, M. *J. Membr. Sci.* **2005**, *263*, 137−145.
(8) Chapotot, A.; Pourcelly, G.; Gavach, C. *J. Membr. Sci.* **1994**, *96*, 167−181.
(9) Kim, Y.; Walker, W. S.; Lawler, D. F. *Water Res.* **2012**, *46*, 2042−2056.
(10) Martí-Calatayud, M. C.; García-Gabaldón, M.; Pérez-Herranz, V. *J. Membr. Sci.* **2012**, *392*−*393*, 137−149.
(11) Chapotot, A.; Lopez, V.; Lindheimer, A.; Aouad, N.; Gavach, C. *Desalination* **1995**, *101*, 141−153.

(12) Sata, T. *Ion exchange membranes: preparation, characterization, modification and application*; The Royal Society of Chemistry: Cambridge, UK, 2004.
(13) Mulyati, S.; Takagi, R.; Fujii, A.; Ohmukai, Y.; Matsuyama, H. *J. Membr. Sci.* **2013**, *431*, 113−120.
(14) Grebenyuk, V. D.; Chebotareva, R. D.; Peters, S.; Linkov, V. *Desalination* **1998**, *115*, 313−329.
(15) Takata, K.; Yamamoto, Y.; Sata, T. *J. Membr. Sci.* **2000**, *179*, 101−107.
(16) Amara, M.; Kerdjoudj, H. *Desalination* **2003**, *155*, 79−87.
(17) Kumar, M.; Tripathi, B. P.; Shahi, V. K. *J. Membr. Sci.* **2009**, *340*, 52−61.
(18) Chamoulaud, G.; Bélanger, D. *J. Colloid Interface Sci.* **2005**, *281*, 179−187.
(19) Tieke, B.; van Ackern, F.; Krasemann, L.; Toutianoush, A. *Eur. Phys. J. E* **2001**, *5*, 29−39.
(20) Decher, G. *Science* **1997**, *277*, 6.
(21) Ahmadiannamini, P.; Li, X.; Goyens, W.; Meesschaert, B.; Vanderlinden, W.; De Feyter, S.; Vankelecom, I. F. J. *J. Membr. Sci.* **2012**, *403−404*, 216−226.
(22) Kochan, J.; Wintgens, T.; Wong, J. E.; Melin, T. *Desalination* **2010**, *250*, 1008−1010.
(23) Abdu, S.; Sricharoen, K.; Wong, J. E.; Muljadi, E. S.; Melin, T.; Wessling, M. *ACS Appl. Mater. Interfaces* **2013**, *5*, 10445−10455.
(24) Lin, H.; Zhao, C.; Ma, W.; Li, H.; Na, H. *Int. J. Hydrogen Energy* **2009**, *34*, 9795−9801.
(25) Malaisamy, R.; Talla-Nwafo, A.; Jones, K. L. *Sep. Purif. Technol.* **2011**, *77*, 367−374.
(26) Sata, T.; Sata, T.; Yang, W. *J. Membr. Sci.* **2002**, *206*, 31−60.
(27) Zabolotsky, V. I.; Nikonenko, V. V.; Pismenskaya, N. D.; Laktionov, E. V.; Urtenov, M. K.; Strathmann, H.; Wessling, M.; Koops, G. H. *Sep. Purif. Technol.* **1998**, *14*, 255−267.
(28) Rubinstein, S. M.; Manukyan, G.; Staicu, A.; Rubinstein, I.; Zaltzman, B.; Lammertink, R. G. H.; Mugele, F.; Wessling, M. *Phys. Rev. Lett.* **2008**, *101*, 236101.
(29) Druzgalski, C. L.; Andersen, M. B.; Mani, A. *Phys. Fluids* **2013**, *25*, 110804-1−110804-17.
(30) Tuan, L. X.; Buess-Herman, C.; Hurwitz, H. D. *J. Membr. Sci.* **2008**, *323*, 288−298.
(31) Pismenskaya, N. D.; Nikonenko, V. V.; Melnik, N. A.; Shevtsova, K. A.; Belova, E. I.; Pourcelly, G.; Cot, D.; Dammak, L.; Larchet, C. *J. Phys. Chem. B* **2011**, *116*, 2145−2161.
(32) Belashova, E. D.; Melnik, N. A.; Pismenskaya, N. D.; Shevtsova, K. A.; Nebavsky, A. V.; Lebedev, K. A.; Nikonenko, V. V. *Electrochim. Acta* **2012**, *59*, 412−423.
(33) Długołęcki, P.; Ogonowski, P.; Metz, S. J.; Saakes, M.; Nijmeijer, K.; Wessling, M. *J. Membr. Sci.* **2010**, *349*, 369−379.
(34) Nikonenko, V. V.; Kozmai, A. E. *Electrochim. Acta* **2011**, *56*, 1262−1269.
(35) Park, J.-S.; Choi, J.-H.; Woo, J.-J.; Moon, S.-H. *J. Colloid Interface Sci.* **2006**, *300*, 655−662.
(36) Sow, P. K.; Sant, S.; Shukla, A. *Int. J. Hydrogen Energy* **2010**, *35*, 8868−8875.
(37) Qaiser, A. A.; Hyland, M. M.; Patterson, D. A. *J. Membr. Sci.* **2011**, *385−386*, 67−75.
(38) Sow, P.; Parvatalu, D.; Bhardwaj, A.; Prabhu, B. N.; Bhaskarwar, A. N.; Shukla, A. *J. Appl. Electrochem.* **2013**, *43*, 31−41.
(39) Park, J. S.; Chilcott, T. C.; Coster, H. G. L.; Moon, S. H. *J. Membr. Sci.* **2005**, *246*, 137−144.
(40) Soboleva, T.; Xie, Z.; Shi, Z.; Tsang, E.; Navessin, T.; Holdcroft, S. *J. Electroanal. Chem.* **2008**, *622*, 145−152.
(41) Tuan, L. X.; Buess-Herman, C. *Chem. Phys. Lett.* **2007**, *434*, 49−55.
(42) Sata, T.; Mizutani, Y. *J. Polym. Sci., Polym. Chem. Ed.* **1979**, *17*, 1199−1213.
(43) Krasemann, L.; Tieke, B. *Langmuir* **1999**, *16*, 287−290.
(44) Urairi, M.; Tsuru, T.; Nakao, S.-i.; Kimura, S. *J. Membr. Sci.* **1992**, *70*, 153−162.
(45) Kotov, V. V.; Peregonchaya, O. V.; Selemenev, V. F. *Russ. J. Electrochem.* **2002**, *38*, 927−929.
(46) Firdaous, L.; Maleriat, J. P.; Schlumpf, J. P.; Quemeneur, F. *Sep. Sci. Technol.* **2007**, *42*, 931−948.
(47) Sata, T.; Yamaguchi, T.; Matsusaki, K. *J. Phys. Chem.* **1995**, *99*, 12875−12882.
(48) Marcus, Y. *Biophys. Chem.* **1994**, *51*, 111−127.
(49) Marcus, Y., *Ion Solvation*; Wiley: Chichester, England, 1985.
(50) Kattan Readi, O. M.; Kuenen, H. J.; Zwijnenberg, H. J.; Nijmeijer, K. *J. Membr. Sci.* **2013**, *443*, 219−226.
(51) Ouyang, L.; Malaisamy, R.; Bruening, M. L. *J. Membr. Sci.* **2008**, *310*, 76−84.
(52) Oren, Y.; Litan, A. *J. Phys. Chem.* **1974**, *78*, 1805−1811.